

Primljen / Received: 10.8.2018.

Ispravljen / Corrected: 27.10.2018.

Prihvaćen / Accepted: 18.12.2018.

Dostupno online / Available online: 10.3.2019.

# Analysis of prefabricated steel dome nodal connection behaviour

## Authors:



<sup>1</sup>Assoc.Prof. **Davor Skejić**  
[davors@grad.hr](mailto:davors@grad.hr)



<sup>2</sup>**Anamarija Alagušić**, MCE  
[anamarija.alagusic@gmail.com](mailto:anamarija.alagusic@gmail.com)



<sup>3</sup>**Gabrijela Hrg**, MCE  
[hrggabrijela@gmail.com](mailto:hrggabrijela@gmail.com)



<sup>4</sup>**Marija Lokin**, MCE  
[marija.lokin7@gmail.com](mailto:marija.lokin7@gmail.com)



<sup>1</sup>Assoc.Prof. **Domagoj Damjanović**  
[ddomagoj@grad.hr](mailto:ddomagoj@grad.hr)

<sup>1</sup>University of Zagreb  
Faculty of Civil Engineering

<sup>2</sup>Intrados projekt d.o.o.

<sup>3</sup>Institut IGH d.d.

<sup>4</sup>Struktura-Projekt d.o.o.

Preliminary note

**Davor Skejić, Anamarija Alagušić, Gabrijela Hrg, Marija Lokin, Domagoj Damjanović**

## Analysis of prefabricated steel dome nodal connection behaviour

The behaviour of a steel geodesic dome node, optimised from the aspect of its assembly, is characterized in the paper. It is an overlap connection with one bolt, where tubular members are flattened and additionally bent to obtain the required dome configuration. Results obtained by means of original laboratory testing and numerical analyses are compared with analytic values determined via simplified expressions for calculation of cross sectional resistance, i.e. govern failure mode. A structural solution is recommended in order to improve this dome connection behaviour and optimise the structure as a whole.

### Key words:

geodesic dome, steel, bolted nodal connection, laboratory testing, numerical analysis, optimisation

Prethodno priopćenje

**Davor Skejić, Anamarija Alagušić, Gabrijela Hrg, Marija Lokin, Domagoj Damjanović**

## Analiza ponašanja čvornog spoja montažne čelične kupole

U radu je karakterizirano ponašanje čvora čelične geodetske kupole koji je optimalan s aspekta montaže. Riječ je o spoju na preklop s jednim vijkom, gdje su cijevni elementi spljošteni i dodatno savinuti da se dobije tražena konfiguracija kupole. Rezultati dobiveni originalnim laboratorijskim ispitivanjem i numeričkim analizama uspoređeni su s analitičkim vrijednostima određenim preko pojednostavljenih izraza za proračun otpornosti kritičnog presjeka, odnosno mjerodavnog načina otkazivanja. Predloženo je konstrukcijsko rješenje s ciljem poboljšanja ponašanja navedenog spoja kupole i optimizacije konstrukcije u cijelosti.

### Ključne riječi:

geodetska kupola, čelik, vijčani čvorni spoj, laboratorijska ispitivanja, numerička analiza, optimizacija

Vorherige Mitteilung

**Davor Skejić, Anamarija Alagušić, Gabrijela Hrg, Marija Lokin, Domagoj Damjanović**

## Analyse des Verhaltens der Knotenverbindung bei vorgefertigten Stahlkuppeln

In der Abhandlung wird das Verhalten der Knoten geodätischer Stahlkuppeln gekennzeichnet, das vom Aspekt der Montage optimal ist. Hierbei handelt es sich um eine Verbindung an der Überlappung mit einer Schraube, wo die Rohrelemente abgeflacht und zusätzlich gebogen sind, um die geforderte Konfiguration der Kuppel zu erreichen. Die durch die ursprünglichen Laboruntersuchungen und numerischen Analysen erhaltenen Ergebnisse wurden mit den analytischen Werten verglichen, die über die vereinfachten Modelle für die Berechnung des kritischen Querschnittswiderstandes beziehungsweise durch relevante Aufhebungsarten ermittelt wurden. Vorgeschlagen wird eine Konstruktionslösung mit dem Ziel, das Verhalten der besagten Kuppelverbindung zu verbessern sowie die Konstruktion im Ganzen zu optimieren

### Schlüsselwörter:

geodätische Kuppel, Stahl, geschraubte Knotenverbindung, Laboruntersuchungen, numerische Analyse, Optimierung

# 1. Introduction

## 1.1. General about geodesic domes

Although the first dome that can be called geodesic was constructed by Walther Bauersfeld, the real father of this type of dome is considered to be Buckminster Fuller. The history of geodesic domes dates back to World War II when they were used as warehouses and for military purposes, but they came to the fore after Fuller designed a dome for the Expo 1967 exhibition in Montreal.

The geodesic sphere is a structure approximately corresponding to an actual sphere, with polygons arranged on its surface, while the geodesic dome is a part of the geodesic sphere [1]. The design of the dome begins with the icosahedron (which consists of twenty equal equilateral triangles) that is entered into a hypothetical sphere. Each triangular part of the icosahedron is divided into  $n^2$  of similar triangular elements, where  $n$  is the chosen degree of division, also called the frequency. There are two-frequency, three-frequency, and multi-frequency domes, and the frequency number itself increases the stability of the dome. Thanks to their stability and aesthetics, geodesic domes are now increasingly competing with other types of structures that are more commonly encountered worldwide. They have been used since the 1950s in the construction of cultural (Figures 1 and 2), housing, and sports facilities [2].



Figure 1. Geodesic dome [4]

Regarding the interior space, a geodesic dome encloses the largest volume of space using the smallest quantity of material

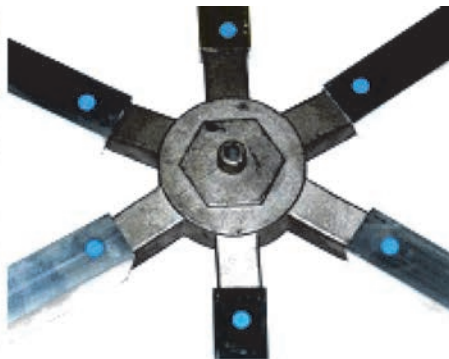


Figure 3. Several solutions of steel geodesic dome nodes [5]

[3]. As a result, it is very light considering the amount of material required for its construction. In addition, the dome geometry itself ensure high level of stability of the entire structure [1]. Such domes are also highly resistant to wind and snow, and can therefore be used in various climatic conditions. The advantage of prefabricated steel domes is that they are lightweight and quick to assemble, while not requiring additional equipment and support during construction work.

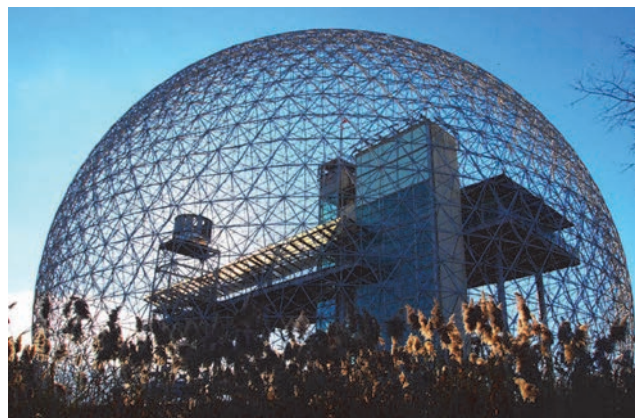


Figure 2. Biosphere, Montreal [1]

## 1.2. Dome node issue

There are several possible solutions for nodes used in steel geodesic domes, such as those shown in Figure 3. The subject of the research proposed in this paper is to present a dome node solution that is optimal from the aspect of erection. This optimal node is formed as a lap connection of 5 to 6 hollow truss members with flattened ends that are bent and interconnected with one bolt, Figure 3.a). A disadvantage of such node solution is the appearance of second-order effects near the connection due to the bending of ends and force eccentricity. Consequently, the resistance of the connection is significantly reduced, compared to the resistance of individual truss members. In order to increase reliability of this kind of dome structures, i.e. to assess behaviour of connecting nodes, a detailed analysis is made of one node element when exposed to tensile and compressive loads. Three approaches or research methods - analytical, experimental, and numerical - are used to determine resistance of this connection [2].

## 2. Analytical assessment of lap node connection resistance

### 2.1. Introduction

Prefabricated geodesic domes are relatively new structural systems and an extensive literature about their design and construction is still unavailable. Solutions used in practice usually result from the aspect of simple erection and are often insufficiently investigated. This type of dome is normally used as a temporary structure, and so there is a need to develop a simple and rapid but sufficiently reliable design to assess its resistance.

In addition to axial force, a bending moment also occurs near the connection of truss elements. This is due to the bending of flattened truss ends and force eccentricity, Table 1. Apart from load direction (tension or compression), the force eccentricity also depends on the configuration of a particular connection. Since there are two possible ways of connecting truss elements in the node, the node resistance is analysed for four distinct cases. Table 1 shows the schemes of all cases, including marked places for forming yielding lines where eccentricities need to be measured.

### 2.2. Analytical calculation of resistance

Generally, there are several characteristic failure modes of bolted shear connections: gross cross-section yield, net tension failure, shear failure of bolts, and bearing failure of the connected member. After analysing this specific type, and configuration of the connection, it was concluded that the failure mode of tension elements is bearing failure, while failure mode of compression elements is bending of flattened part of tube element, i.e. formation of a plastic mechanism.

Since the eccentricity of tensile elements decreases with an increase in axial force, the applicable failure mode becomes the bearing failure in a flattened part of tube around bolt,  $F_b$ . According to EN 1993-1-8 [6],  $F_b$  can be calculated as:

$$F_b = k_1 \cdot a_b \cdot f_u \cdot d \cdot t \tag{1}$$

where:

$k_1$  - the reduction coefficient perpendicular to the direction of load transfer (see Table 3.4 [6])

Table 1. Eccentricity depending on force direction and element position in node connection

Tension (T1)	Compression (C1)
Tension (T2)	Compression (C2)

Symbols used in schemes are defined as follows:  
 L - length of flattened end of tube element, a - length of connection lap,  $\alpha$  - slope angle of flattened end of tube element,  $h_w$  - bolt head diameter, t - thickness of tube element, e - eccentricity

- $a_b$  - the reduction coefficient parallel to the direction of load transfer (see Table 3.4 [6])
- $f_u$  - the ultimate tensile strength of steel
- d - the bolt diameter
- t - the thickness of the element at the bolt hole location.

The compression element exhibits a completely different behaviour. Unlike the tensile element, in this case the eccentricity increases with an increase in force, and the applicable failure mode becomes the deflection of bent flattened tube part. Therefore, a yield mechanism forms between the start of the bent flattened part and centre of rotation around other node elements, see cases (C1) and (C2) in Table 1. In practice, a simplified theoretical interaction expression is used to calculate the critical cross-sectional resistance of the bent flattened tube part of the compression element.

Based on general interaction expressions, the resistance of cross section to axial force and bending moment (which derives from eccentricity) is defined according to EN 1993-1-1 [7]. The axial resistance that takes into account the effect of eccentricity can be expressed by:

$$N'' = \frac{1}{1/A + e/W_{pl}} \cdot f_y \tag{2}$$

where:

- A - the area of the flattened tube cross section
- $W_{pl}$  - the plastic resistance moment of the flattened tube part
- e - eccentricity, Table 1, cases (C1) and (C2)
- $f_y$  - the steel yield strength.

These analytical expressions, confirmed in practice a long time ago, provide reliable resistance values that are on the side of safety. However, node connection resistances obtained by these expressions are significantly lower compared to buckling resistance of the structural element that is being connected [2]. The question arises whether it is a conservative approach, or this kind of node solution can withstand significantly lower force than the connecting element itself. These preliminary analytical considerations were the motivation for the comprehensive laboratory testing and additional numerical simulations of this characteristic connection behaviour [2].

### 3. Laboratory testing of dome node connection

#### 3.1. Scope and objectives of laboratory testing

The laboratory testing of the bolted node connection behaviour was conducted at the Structural Testing Laboratory of the Faculty of Civil Engineering in Zagreb. Due to complexity of the procedure, the testing involved the real node configuration, a simplified version with one element and a thick steel plate, representing other elements of the connection. This simplified configuration was selected to provoke failure of the critical flattened and additionally bent section of the tube element near the connection. Test specimens were classified into two groups depending on the load, i.e. group T (*Tension*) and group C (*Compression*). Each group consisted of three specimens, and so six specimens in total were tested.

#### 3.2. Geometry and mechanical properties of tube specimens

All specimens consist of a 42.2 x 2.0 mm circular hollow (tube) member that is bolted to a 20 mm thick steel plate. The mean measured value of the tube wall thickness is 1,9 mm. Actual properties of the material were determined by tensile test conducted according to EN ISO 6892-1 [8]. Six test

pieces of the tube were tested. The stress – strain diagrams describing their behaviour are shown in Figure 4. Although the nominal steel quality should have been S235, it was experimentally established that the strength of steel and its yield strength are higher. The observed increase in material strength properties as well as the characteristic shape of the diagram can be related to the cold-formed production process of tube elements. A mean values of yield stress, 417 MPa, and strength, 461 MPa, where obtained by the processing of experimental results. The nominal value of 210000 MPa was adopted for elastic modulus.

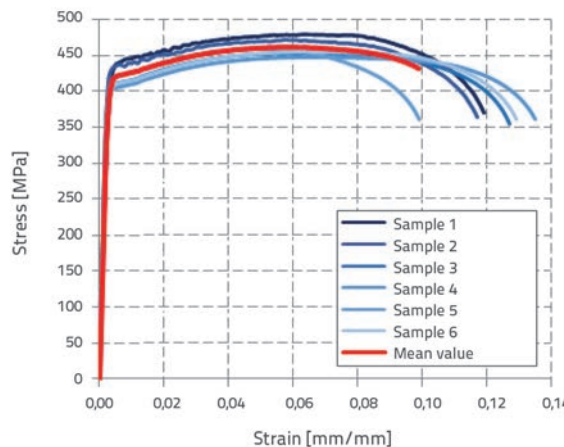


Figure 4. Stress-strain ( $\sigma$ - $\epsilon$ ) diagrams of steel tubes

#### 3.3. Test procedure

At one end, the tube element was flattened and bent to an angle of 12°. The plate was fixed at the same angle with two trapezoidal stiffeners on each side, Figure 5. At the other end, the tube member was also strengthened with trapezoidal stiffeners perpendicular to one another, Figure 6.

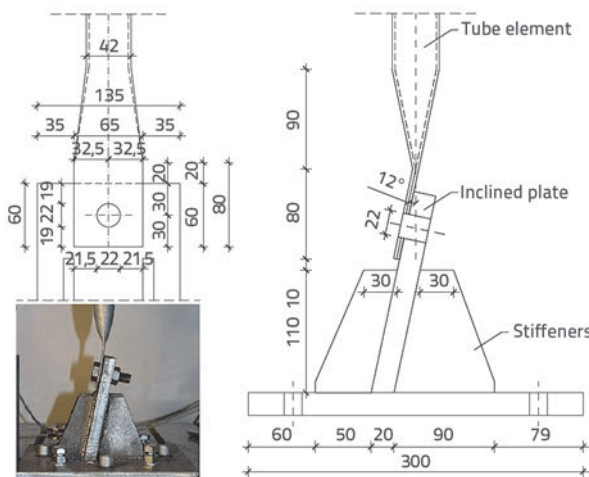


Figure 5. Tube element to support connection detail (simulation of node connection)

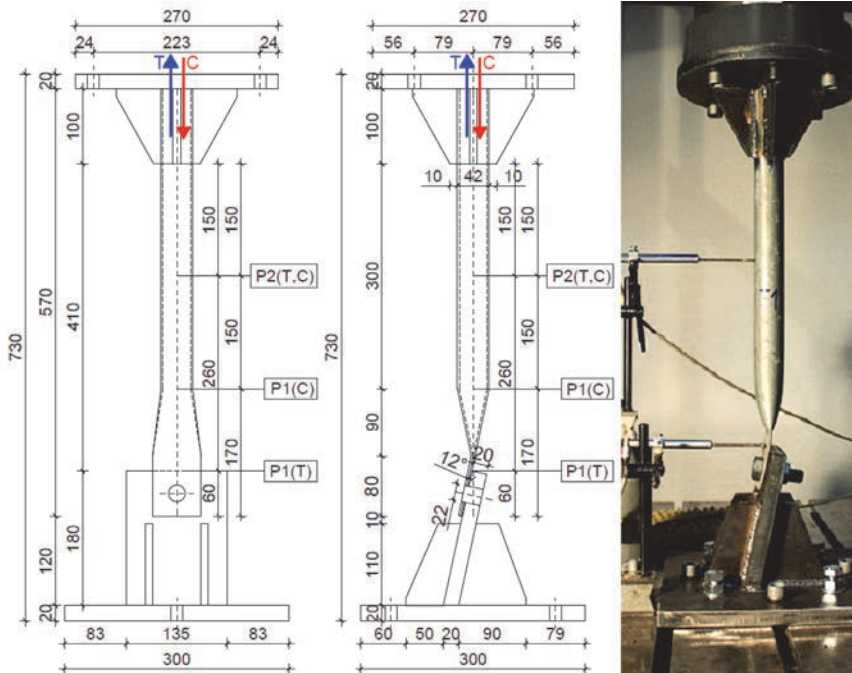


Figure 6. Positions of measuring points during experimental testing

The testing was performed using the Zwick&Roell static testing machine with the capacity of  $\pm 600$  kN. The specimens were first tested to tension (T1, T2, and T3), and then to compression (C1, C2, and C3). The load was applied by the testing machine according to Figure 6, and the tests were conducted in the displacement control mode, at the speed of 0,5 mm/min, in the elastic region. After entering the plastic region, the speed was increased to 2 mm/min until specimen failure. Horizontal displacements were measured by LVDT sensors in two points. For tensile specimens, LVDTs were placed 60 mm from the lower edge of tube element (position P1(T)), and 150 mm from the edge of upper stiffeners (position P2). After tension testing, the specimens were tested to compression. After the first compression specimen testing, the measuring device was moved from position P1(C) above the bolt to the distance of 150 mm from P2, i.e. 170 mm from the bottom edge of the tube, as shown in Figure 6.

### 3.4. Test results and specimen behaviour

Force-displacement diagrams for two measuring points P1 and P2 and force-stroke (testing machine) diagrams were experimentally obtained. Figure 7 shows the force-stroke diagrams for all tested specimens. Unlike tension (T), the compression specimens (C) exhibit significant differences in behaviour. The observed differences, especially the deviation of specimen C1, are due to initial differences in geometry when bending the tube end, and when assembling the specimens. By analysing displacements and maximum forces of the tensile and compression specimens, it can be concluded that specimens can withstand force that is approximately 10 kN higher when tested in tension. However, strokes of tensile specimens are also significantly higher. The failure mode was also determined by experimental testing. Under the

tensile load, the tube straightened so that the bent section coincided with the element axis. Additionally, with the tensile load applied on the upper side of the specimen, the specimen was pulled upward, and it pressed the bolt leading to fracture at its lower edge, Figure 8.a). Thus, the ultimate failure of tensile specimens occurred due to bearing around the bolt hole because the effect of eccentricity disappeared with the straightening of the specimen. In case of compression specimens, the flattened section of the tube element bended over the lower inclined plate that simulated other members connected at the dome node, Figure 8.b). The bending progressed by formation of two yield lines, i.e. of the plastic mechanism, at the moment of specimen failure. Thus, the failure of compression specimens occurred by bending caused by initial eccentricity of the flattened section of the tube member, which was continuously increasing thus accelerating the formation of plastic mechanism.

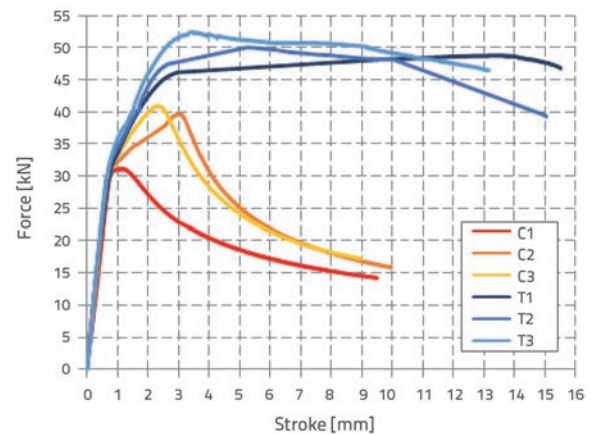


Figure 7. Force-stroke (testing machine) diagrams for both tensile and compression specimens

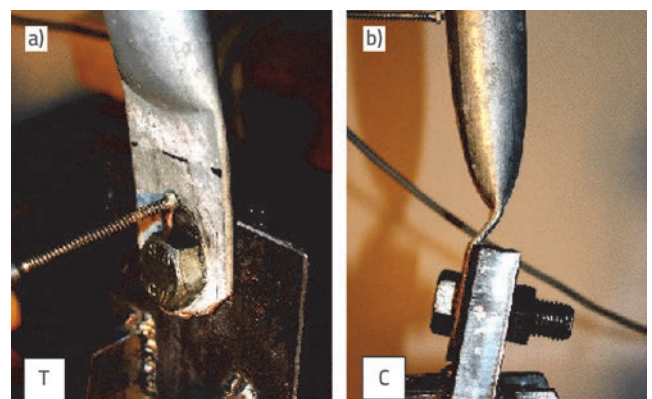


Figure 8. Failure modes: a) tensile specimen (T); b) compression specimen (C)

### 3.5. Characterization of specimen behaviour

The initial stiffness, resistance, ultimate resistance and displacements corresponding to individual resistances, are determined based on force-displacement diagrams (Figure 7). Mean mechanical characteristics of tensile and compression specimens are shown in Table 2. The experimental curves characterization procedure is explained in greater detail in [2].

Table 2. Characterization results of force-stroke curves (mean values) [2]

Specimen	$S_{ini}$ [kN/m]	$N_R$ [kN]	$u_R$ [mm]	$N_u$ [kN]	$u_{Nu}$ [mm]	$u_u$ [mm]
Tension (T)	47217	46.0	1.04	50.4	7.37	14.8
Compression (C)	45013	32.6	0.75	37.3	2.17	9.48

In Table 2,  $S_{ini}$  represents the initial stiffness,  $N_R$  is the resistance obtained as the intersection of the secant of elastic region and the post-critical region up to ultimate resistance,  $u_R$  is the displacement corresponding to  $N_R$ ,  $N_u$  represents the ultimate resistance and  $u_{Nu}$  is the corresponding displacement. The ultimate displacement at fracture is  $u_u$ .

### 4. Numerical simulation of dome connection behaviour

#### 4.1. General

A numerical simulation of the dome node connection behaviour under compression and tension load is presented in this section. The dome connection is modelled by means of the finite element method using the simulation program ANSYS 15.0 [9]. The numerical modelling of this problem is complex because it requires defining an appropriate geometry of joint, material properties, support conditions, contacts, and loading conditions. The analysis also considers second-order effects, plasticity of material, and one-way contact boundary conditions. The actual behaviour of the tube material is simulated by an isotropic

multilinear model obtained on the basis of tensile test results (Figure 4). The numerical model is calibrated and evaluated through comparison with results obtained by laboratory testing.

#### 4.2. Description of finite element models

Three-dimensional models of finite elements (FE models) were used for simulation of the force-displacement (F-Δ) behaviour of specimens subjected to tension and compression. Volume elements in the form of tetrahedron with 10 knots, SOLID187 [9], were used. Detailed parametric analyses were conducted in order to calibrate a model that can efficiently simulate the F-Δ response of connection of dome tube elements subjected to tension and compression in relation to laboratory tests.

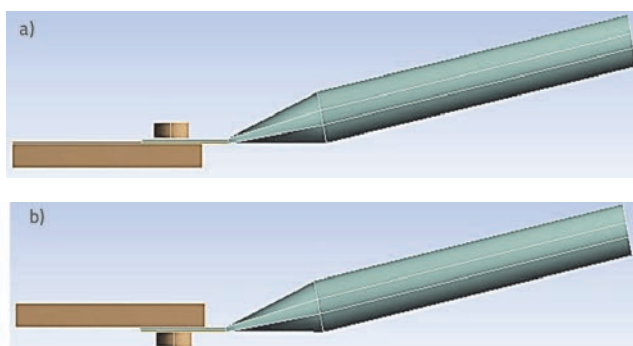
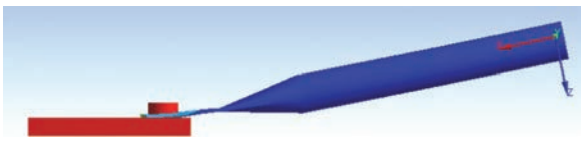
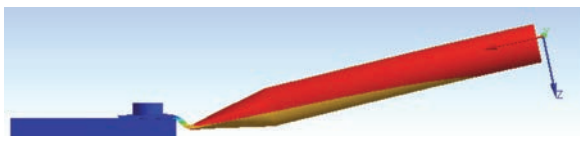
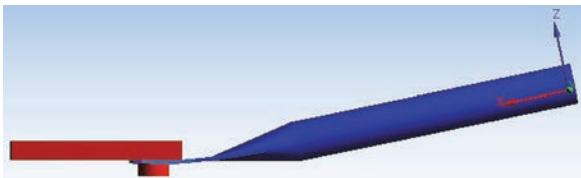
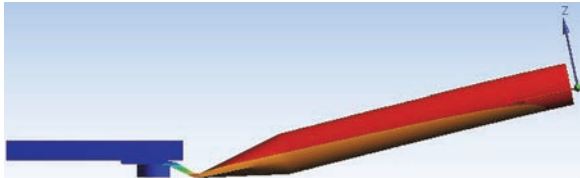


Figure 9. Analysed connection configurations

Based on laboratory tests, two numerical models were calibrated depending on the load direction (tension or compression). Since only one geometric configuration in tension and compression was tested in laboratory, the other configuration of the connection was analysed with two additional numerical models depending on load direction, Figure 9. The first configuration was modelled with the disposition of elements identical to that of laboratory specimens, Figure 9.a). In the second configuration, the tube

Table 3. Deformed shapes of analysed 3D finite element model

Configuration 1	
FEM_T1	FEM_C1
	
Configuration 2	
FEM_T2	FEM_C2
	

element was connected to the other side of the node plate, Figure 9.b). The total of four distinct models were analysed and every one of them consisted of a tube element, connection steel plate, and bolt M 20. The aim of numerical analysis of various models was to investigate the influence of force eccentricity on the resistance of this type of connection.

Deformed models after simulation are presented in Table 3. Both configurations were tested to tensile load (FEM\_T1 and FEM\_T2) and compression load (FEM\_C1 and FEM\_C2). It can be concluded that tensile specimens fail by bearing and compression specimens fail by bending of the bent flattened tube part, which is in line with experimental findings.

### 4.3. Numerical results and discussion

Force to displacement curves (F- $\Delta$  curves), which describe the total behaviour of the observed models subjected to tensile and compression loads, were obtained as a result of numerical analysis. The comparison between numerical simulation results of the configuration 1 connection and results obtained with laboratory tests are presented separately for the tensile and compression load in Figures 10 and 11.

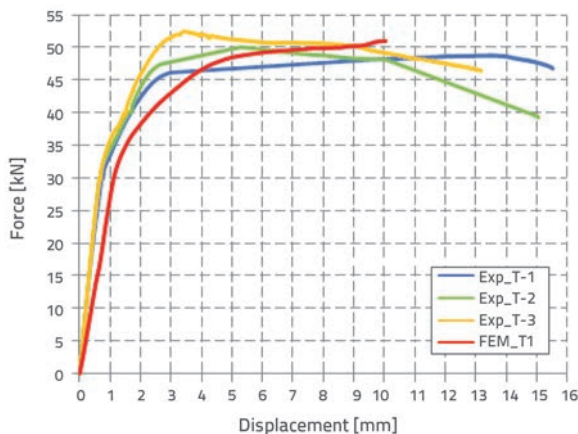


Figure 10. Comparison between numerical (FEM) and laboratory (Exp) F- $\Delta$  curves for first connection configuration subjected to tensile load (T)

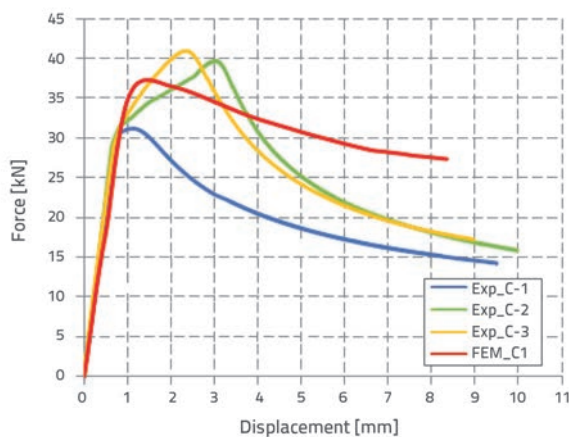


Figure 11. Comparison between numerical (FEM) and laboratory (Exp) F- $\Delta$  curves for first connection configuration subjected to compression load (C)

The results obtained by numerical simulations coincide well with experimental results. In case of tensile load of the connection, the numerical simulations give a somewhat softer response when compared to laboratory tests (Figure 10). This difference can be explained by different bolt positions and friction effects, which were maximally simplified in numerical simulations. Namely, the initial contact between the element and the bolt was assumed, and the friction effect was neglected. As can be seen in Figure 11, numerical results for compression loaded connection coincide very well in elastic area with experimental results for all three specimens. Although a greater deviation of results occurs in post-critical area, that is not considered crucial for characterization of connection behaviour.

Numerical results obtained by simulations for all four models, depending on the configuration of connection and load direction, are compared in Figure 12.

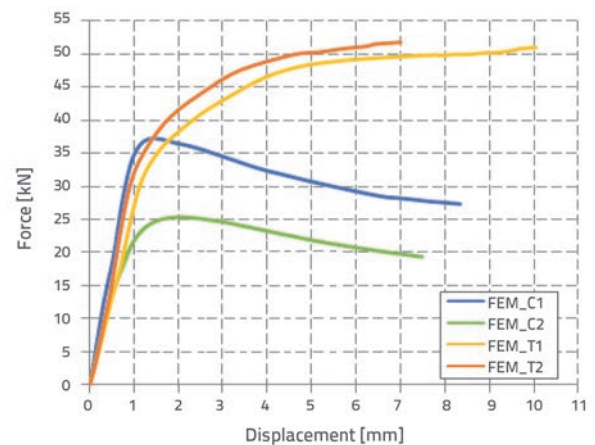


Figure 12. Comparison of numerical (FEM) simulations of behaviour of all analysed models

Based on results obtained by numerical simulations, it was concluded that failure mode of the compression element with configuration 2 in form of bending of flattened tube part is the most relevant for the resistance of node connection, Table 3, (FEM\_C2). The reason for that is the highest eccentricity of axial force that causes the appearance of highest bending moments and significant reduction of the compression element resistance in connection.

## 5. Discussion of results and proposal of a new solution

### 5.1. Comparison of resistances

The resistance of the bolted node connection for all four analysed cases (two configurations and two load directions) is obtained by analytical, experimental and numerical methods. The corresponding values are summarized in Table 4. It should be noted that the analytical resistances are calculated with the mean values of measured geometric and mechanical properties, see Section 3.2.

Table 4. Summary of dome node connection resistances

Method	Tension [kN]		Compression [kN]	
	AN_T1	AN_T2	AN_C1	AN_C2
Analitička (AN)	42.0	42.0	29.3	14.9
	AN/Exp [%]			
Experimental (Exp)	Exp_T1	-	Exp_C1	-
	46.0	-	32.6	-
	AN/Exp [%]			
Numerical (FEM)	FEM_T1	FEM_T2	FEM_C1	FEM_C2
	47.0	47.5	35.9	21.4
	AN/FEM [%]			
	12.0	11.6	18.4	30.4

As expected, experimental and numerical resistance values of the analysed connection are higher than those obtained through analytical expressions. Deviations are not significant in case of the tension element, and a high compatibility of resistance values obtained by all three methods can be observed. Experimental and numerical analyses of the connection behaviour revealed that the tension element is straightening, which means that the eccentricity and second-order effects are decreasing. Based on these observations, it is suggested to neglect the effect of bending moment in the analytical expression and to calculate the resistance based on axial force only. In this way, the resistance of the tension element increases significantly, and the proper failure mode is the bearing failure around the bolt. For that reason, the resistance to bearing failure for tension elements with both configurations was determined using expression (1). On the other hand, the compression element bends further, thereby increasing the eccentricity and causing an additional bending moment. The bending of the flattened part of tube occur faster. The analytical expression provides acceptable resistance values for compression elements, but it is necessary to determine the associated values of initial eccentricity considering the connection configuration. Deviations of analytical results from those obtained by experimental method (8% for tension element and 10% for compression element) are slightly smaller compared to deviations from numerical results. However, the maximum deviation occurs at the compression element with second connection configuration, which amounts to 30,4%.

## 5.2. Proposal of new node connection solution

### 5.2.1. New node configuration

Based on the analyses, a new node design solution, involving connection of the straight flattened tube end sections to a specially shaped steel plate, is proposed, as shown in Figure

13. Adverse effects of eccentricity and second-order effects are annulled in this way. In order to demonstrate the effectiveness of such solution, without considering a somewhat complicated production, additional numerical models were made, Figure 14. The characterization of their behaviour was performed based on the results of this analysis.

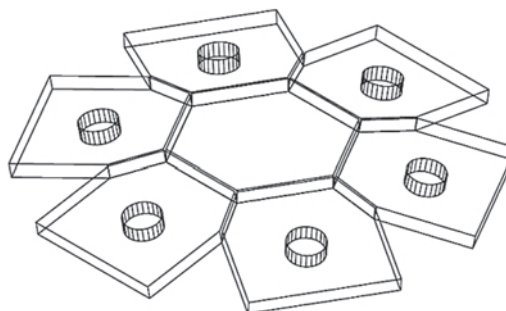


Figure 13. Principal proposal of solution for node plate

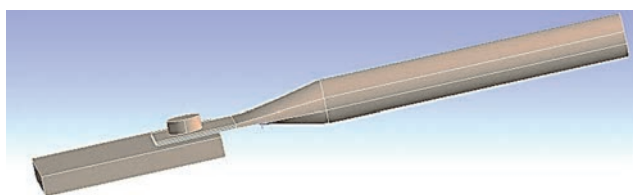


Figure 14. Numerical model of new node-connection solution (same for tension and compression)

### 5.3. New connection configuration analysis

After numerical analysis of the new node solution, the corresponding F-Δ curves were created to show behaviour of connection elements subjected to tension load (FEM\_T\_corr) and compression (FEM\_C\_corr) load. The behaviour of new connection configuration was compared with relevant behaviour of traditional solution, separately for tension, Figure 15, and compression, Figure 16.

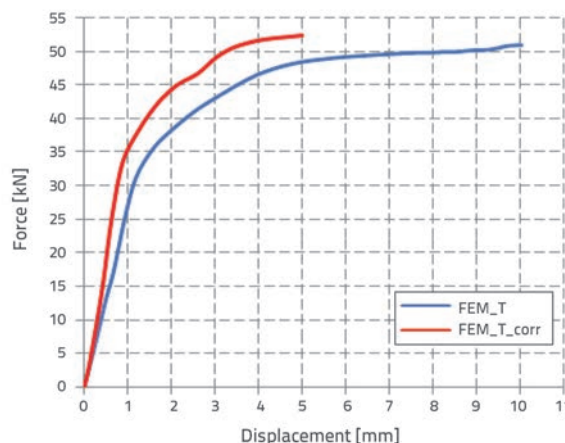


Figure 15. Comparison of analysed connection with new solution for tension elements

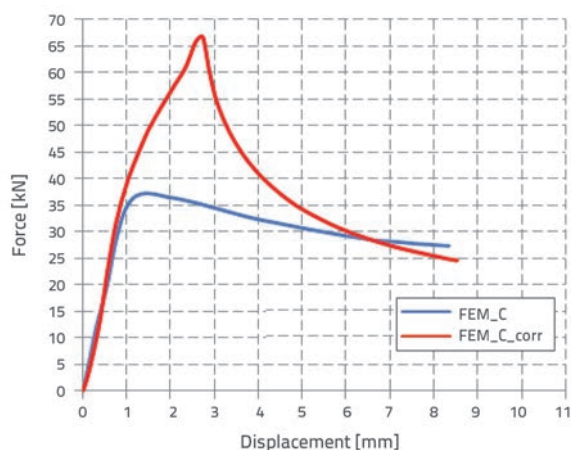


Figure 16. Comparison of analysed connection with new solution for compression elements

Although an increase in initial stiffness of the new solution for tension element can be detected, Figure 15, it can also be concluded that the change of element configuration in node connection does not significantly affect the resistance ( $FEM\_T\_corr/FEM\_T1 = 48.1/47.0 = 1.02$  times). This confirms the fact that bending of the flattened part of an element does not have a significant impact on the behaviour of tension elements and that the elements strained in such a way fail by bearing failure around the bolt. On the other hand, approximately 2.66 times higher compression resistance was obtained by straightening tube element, compared to the previously analysed critical numerical model ( $FEM\_C\_corr/FEM\_C2 = 57.0/21.4$ ). Thereby, the problem of adverse effects of additional bending moment caused by eccentricity, i.e. by bent flattened tube part, is solved. Since the failure mode of the new node connection solution also changes, the actual increase in resistance exhibited by the new solution amounts to 2.25 times ( $FEM\_T\_corr/FEM\_C2 = 48.1/21.4$ ).

## 6. Conclusion

Comparison of analytical, experimental and numerical results reveals that analytical method is reliable for assessing resistance

of the analysed node connection for a geodesic dome. However, the ingrained analytical assessment of compression resistance, expression (2), is quite incomplete. Namely, in practice, the existence of eccentricity caused by bending of the flattened tube part is taken into account regardless of direction of internal force (compression or tension). Furthermore, this simple analytical expression neglects the real position of the element in the connection (internal, central or external).

Actual force-displacement curves, which completely define the behaviour of this kind of connection, were obtained by laboratory testing. It was noticed that results coincide well with proposed analytical expressions in case of compression load, and with the existing expressions for bearing failure, in case of tension load.

Based on the results obtained by laboratory testing, numerical models (FEM) were calibrated using the numerical program ANSYS 15.0 [9]. These models served for an additional numerical parametric analysis where the position of connection elements, that is node configuration, was varied. It was numerically confirmed that the way the connection is established, i.e. the design of a particular type of node connection, has a significant impact on resistance, and that analytical expressions must consider the most unfavourable position of the compression element in the connection.

Relevant failure modes were determined by the analysis and comparison of results, and a new node configuration solution was proposed. This new solution considers a somewhat more complicated production of node plates, but it annuls adverse effects of eccentricity and second-order effects. Such node design results in element failure by bearing failure, and an increase in resistance of 2.25 times is achieved compared to the solution with a bent flattened tube part. However, such node solution requires a form that is somewhat more complicated. On the other hand, as the node plate is characterised by a relatively small thickness, it can be fabricated by the cold forming process, which is not so costly.

Since only one element was experimentally tested, it is recommended to extend this research. It would be useful to test behaviour of a real node in one field or in a real dome in order to further confirm its effectiveness and optimize the proposed solution.

## REFERENCES

- [1] Horvat, M.: Structural project of prefabricated steel geodesic dome 3v7, University of Zagreb, Faculty of Civil Engineering, graduate thesis, Zagreb 2016, [in Croatian].
- [2] Alagušić, A., Hrg, G., Lokin, M.: Behaviour characterization of the steel geodesic dome node, University of Zagreb, Faculty of Civil Engineering, Student work for the Rector prize, Zagreb, 2017, [in Croatian].
- [3] Sieden, L. S.: The birth of the geodesic dome; how Bucky did it, *The Futurist*, 26 (1989) 6, pp. 14-18.
- [4] <http://www.kupole.hr>, accessed 13 February 2018
- [5] <http://www.domerama.com>, accessed 08 January 2017
- [6] EN 1993-1-8:2014, Eurocode 3: Design of steel structures - Part 1-8: Design of joints (EN 1993-1-8:2005+AC:2009)
- [7] EN 1993-1-1:2014, Eurocode 3: Design of steel structures - Part 1-1: General rules and rules for buildings (EN 1993-1-1:2005+AC:2009)
- [8] EN ISO 6892-1:2016, Metallic materials – Tensile testing – Part 1: Method of test at room temperature (ISO 6892-1:2016; EN ISO 6892-1:2016)
- [9] ANSYS, Users Manual (Version 15.0), Houston, TX, USA, Swanson Analysis Systems Inc., 2013.